

This document is confidential and is proprietary to the American Chemical Society and its authors. Do not copy or disclose without written permission. If you have received this item in error, notify the sender and delete all copies.

New insights from zinc and copper isotopic compositions of atmospheric particulate matter from two major European cities

Journal:	<i>Environmental Science & Technology</i>
Manuscript ID	es-2016-008639.R2
Manuscript Type:	Article
Date Submitted by the Author:	30-Jul-2016
Complete List of Authors:	Ochoa González, Raquel; Imperial College London, Earth Science and Engineering Strekopytov, Stanislav; Natural History Museum, Mineralogy AMATO, FULVIO; CSIC, Querol, Xavier; CSIC-IDAEA, Geosciences Reche, Cristina; Institute for Environmental Assessment and Water Research (IDÆA-CSIC), Weiss, Dominik; Imperial College London, Earth Science and Engineering

SCHOLARONE™
Manuscripts

1
2
3
4
5
6
7
8
9
10
11
12
13
14
15
16
17
18
19
20
21
22
23

New insights from zinc and copper isotopic compositions of atmospheric particulate matter from two major European cities

R. Ochoa Gonzalez,^{1*} S. Strekopytov,² F. Amato³, X. Querol,³ C. Reche³ and D. Weiss¹

¹Department of Earth Science and Engineering, Imperial College London, London, SW7 2AZ, UK

²Imaging and Analysis Centre, Natural History Museum, London, SW7 5BD, UK

³Institute of Environmental Assessment and Water Research, Barcelona, 08034, Spain

*Corresponding author: r.ochoa-gonzalez@ic.ac.uk; d.weiss@imperial.ac.uk

Phone: +44 (0)20 7594 6383

24 Keywords: Zn and Cu isotopes, source apportionment, particulate matter, traffic pollution,
25 MC-ICP-MS, atmospheric environment

26

27 Abstract

28 This study reports spatial and temporal variability of Zn and Cu isotopes in atmospheric
29 particulate matter (PM) collected in two major European cities with contrasting atmospheric
30 pollution, Barcelona and London. We demonstrate that non-traditional stable isotopes
31 identify source contributions of Zn and Cu and can play a major role in future air quality
32 studies.

33 In Barcelona, fine PM were collected at street level at sites with variable traffic density.
34 The isotopic signatures ranged between -0.13 ± 0.09 and -0.55 ± 0.09 ‰ for $\delta^{66}\text{Zn}_{\text{IRMM}}$ and
35 between $+0.04 \pm 0.20$ and $+0.33 \pm 0.15$ ‰ for $\delta^{65}\text{Cu}_{\text{AE633}}$. Copper isotope signatures similar to
36 Cu sulphides and Cu/Sb ratios within the range typically found in brake wear suggest that
37 non-exhaust emissions from vehicles are dominant. Negative Zn isotopic signatures
38 characteristic for gaseous emissions from smelting and combustion and large enrichments of
39 Zn and Cd suggest contribution from metallurgical industries.

40 In London, coarse PM collected on the top of a building over 18 months display isotope
41 signatures ranging between $+0.03 \pm 0.04$ and $+0.49 \pm 0.02$ ‰ for $\delta^{66}\text{Zn}_{\text{IRMM}}$ and between
42 $+0.37 \pm 0.17$ and $+0.97 \pm 0.21$ ‰ for $\delta^{65}\text{Cu}_{\text{AE633}}$. Heavy Cu isotope signatures (up to
43 $+0.97 \pm 0.21$ ‰) and higher enrichments and Cu/Sb ratios during winter time suggest important
44 contribution from fossil fuel combustion. The positive $\delta^{66}\text{Zn}_{\text{IRMM}}$ signatures are in good
45 agreement with signatures characteristic for ore concentrates used for the production of tires
46 and galvanised materials, suggesting non-exhaust emissions from vehicles as the main source
47 of Zn.

48

49 1. Introduction

50 Source identification using trace metals in atmospheric particulate matter (PM) is key to air
51 quality programmes in major cities around the world.¹ Different techniques such as principal
52 component analysis and positive matrix factorization are typically applied,^{1, 2} but they require
53 in general the statistical analysis of multi-elemental datasets containing large number of
54 samples collected over long periods. Therefore, the recently explored application of non-
55 traditional stable isotopes for source identification of metal pollutants in the atmosphere is of
56 great interest as it requires smaller sets of samples.³

57 Previous work found that the main sources of Zn in atmospheric PM are emissions
58 from incineration, metal production, fossil fuel combustion and non-exhaust sources from
59 road traffic.^{4, 5} ZnO is the dominant species emitted from tire-treads⁶ and has been identified
60 in emissions from metal smelting along with ZnS.⁷ Copper has likewise been linked to
61 multiple sources, including smelting, oil combustion, wood smoke and brake wear.^{4, 8, 9}
62 Copper typically occurs as oxide, silicate and carbonate, and is often associated with the
63 organic fraction in PM.^{5, 10}

64 The Zn isotope composition relative to the widely used standard JMC 3-0749L Lyon
65 (expressed generally as $\delta^{66}\text{Zn}_{\text{Lyon}}$) is mostly positive in igneous rocks, ranging between +0.2
66 and +0.5‰ in basalts and between +0.4 and +0.6‰ in more acidic rocks, e.g. in granodiorites
67 and granites.¹¹ The $\delta^{66}\text{Zn}_{\text{Lyon}}$ of sphalerite, the major source of Zn concentrates used for
68 industrial purposes, ranges typically between -0.04 and +0.30‰.¹²⁻¹⁴ In contrast, combustion
69 and smelting processes seem to produce lighter (up to -0.52 ‰) and heavier Zn (up to
70 +1.49‰) in the flue gas and residues, respectively.^{13, 15, 16} These values are outside the natural
71 range of Zn isotope signatures and this is likely due to evaporation and condensation
72 processes.¹⁶ Ore tailings collected from a smelter and fly ash in different coal-fired power
73 plants had $\delta^{66}\text{Zn}_{\text{Lyon}}$ values as heavy as +1.49‰.^{13, 16, 17} Previous work on Zn isotopes in PM
74 collected in industrial, urban and remote areas showed indeed significant isotopic variability
75 with $\delta^{66}\text{Zn}_{\text{Lyon}}$ ranging from -1.13 to +0.33‰, suggesting that different sources and
76 anthropogenic activities impart a distinctive isotopic composition to PM.^{15, 18-20} Zinc in PM
77 smaller than 10 μm (PM_{10}) emitted from a refinery in northern France imparted light isotope
78 signatures with $\delta^{66}\text{Zn}_{\text{Lyon}}$ ranging between -0.52 and +0.02‰.¹⁵ Light Zn was also identified
79 in PM collected in São Paulo, with $\delta^{66}\text{Zn}_{\text{Lyon}}$ ranging between -1.05 and -0.46‰ in $\text{PM}_{2.5-10}$
80 and between -1.13 and -0.07‰ in $\text{PM}_{2.5}$.¹⁹ The isotopic composition of PM_1 collected over
81 the equatorial eastern North Atlantic region had $\delta^{66}\text{Zn}_{\text{Lyon}}$ signatures ranging between
82 +0.03±0.04‰ and +0.17±0.10‰.¹⁸ These values are not significantly different from the
83 isotopic signatures of natural sphalerite but lighter than PM_4 separated from soil dust
84 collected from the Sahel region, ranging between +0.23±0.05‰ and +0.28±0.08‰.^{12, 13, 18}
85 Atmospheric PM collected over the North Atlantic Ocean exhibited $\delta^{66}\text{Zn}_{\text{Lyon}}$ between
86 +0.13±0.08 and +0.54±0.08‰ which falls within the range found for igneous rocks.²¹ In
87 summary, Zn in natural materials including igneous rocks and minerals used in the
88 production of ore concentrates likely has an isotope fingerprint between +0.2 and +0.6‰,
89 while residues and particles produced by smelting, refining and combustion processes have
90 isotope signatures outside this range.

91 Copper isotopes were investigated for their potential to identify source contributions in
92 surface and groundwater, and in soils near mines or smelters.²²⁻²⁶ The average Cu isotope
93 composition expressed as $\delta^{66}\text{Cu}_{\text{NIST976}}$ for chalcopyrite (CuFeS_2) is +0.32±0.04‰.²⁷ The
94 $\delta^{65}\text{Cu}_{\text{NIST976}}$ values in other natural minerals vary between -16.96 and +9.98‰, but most
95 signatures fall within the range of -1.5 and +2.5‰.^{22, 27-30} Copper isotope signatures are
96 variable within and between mineral groups, including native Cu or Cu sulphides and
97 carbonates.²⁷ Studies assessing the potential of Cu isotopes for tracing source contributions
98 in the atmosphere are scarce. The $\delta^{66}\text{Cu}_{\text{NIST976}}$ values in PM_1 collected over the North
99 Atlantic Ocean (West Africa) ranged between -0.14±0.09 and -0.02±0.10‰.¹⁸ These
100 signatures were slightly more negative than the isotopic signatures in Sahel soil dust, which
101 ranged between +0.03±0.12 and +0.20±0.16‰.¹⁸ The Cu isotope signatures in PM collected
102 over the North Atlantic Ocean ranged between -0.18±0.11 and +0.30±0.11‰.²¹ Changes in
103 mineralogy and mixing with industrial emissions from North Africa were suggested as
104 possible mechanisms for the variability of Cu isotope signatures.^{18,21}

105 Emissions from fossil fuel combustion are likely more important during winter in
106 Europe and soil dust and non-exhaust vehicle emission sources (tires, brakes or brake discs)
107 are likely to dominate during spring and summer.³¹ Therefore, significant temporal
108 variability in source contributions of trace metals is expected in urban PM. This should be
109 reflected in the Zn and Cu isotope signatures in PM collected during different seasons. This
110 hypothesis, however, has not been tested before and, indeed, there is a lack of knowledge on
111 both the spatial and temporal variability of Zn and Cu isotopes in atmospheric PM.

112 The aim of this study was to assess spatial, and short and long temporal variations of Zn
113 and Cu isotope signatures in PM collected in Barcelona and London and to test associations
114 with pollution sources. London and Barcelona have been selected in this study due to their
115 contrasting sources of metals in PM following the findings of previous studies.³²⁻³⁴ In
116 London, studies based on particle size distributions and traffic tracers (Cu, Fe, Sb and Ba)
117 indicate that the sources of PM are dominated by non-exhaust traffic emissions from
118 vehicles; in Barcelona, metallurgical emissions, characterised mainly by high Pb and Zn
119 concentrations, contribute significantly to the metal burden of the city.³²⁻³⁴ To this end, we
120 first determined the spatial and short-term temporal variability of Zn and Cu isotope
121 signatures in PM₁₀ collected at sites with low and high traffic density at street level over two
122 sampling campaigns during autumn of 2012 and spring of 2013 in Barcelona. Long-term
123 seasonal variability, and hence possible influence of fuel burning, at elevated heights was
124 evaluated using continuous sampling of PM_{2.5-80} during 18 months in London. Enrichment
125 factors (EF) of elemental tracers for non-exhaust traffic emissions (Fe for brake discs and Sb
126 for brakes) and for metallurgical emissions (Cd),⁷ were determined to assist possible source
127 attribution. Finally, the results were compared with previously reported Zn and Cu isotope
128 signatures in atmospheric and anthropogenic PM to critically assess if it is possible to
129 pinpoint anthropogenic sources.

130

131 **2. Materials and Methods**

132 *Sample collection and digestion*

133 In Barcelona, PM₁₀ were sampled at street level at sites located in areas with high and low
134 traffic using high volume samplers (MCV PM1025 and DIGITEL DH80) for 24 or 48 h on
135 quartz fiber filters (Ø15 cm, Pallflex or Munktell). Filters were collected at a height of 3 m
136 over a period of three weeks during two sampling campaigns in 2012 and 2013. Twelve
137 samples were collected at Torre Girona (B1-B6) and Corsega Avenue (T1-T6) during
138 February and March 2012, and eight samples at Palau Reial (B7-B10) and Valencia Avenue
139 (T7-T10) during June 2013. Valencia Avenue and Corsega Avenue are the high traffic sites
140 (14,000 and 11,000 veh day⁻¹, respectively). Torre Girona and Palau Reial represent sites
141 with low traffic and are situated 20 km away from a metallurgical industry. A map showing
142 the monitoring locations and further information about the studied area is given in the
143 Supporting Information (Figure S1). Half of each filter was digested using 2.5 ml of 16 M
144 HNO₃ and 5 ml of 28 M HF in PFA vials (Savillex, MN, USA) at 140 °C on a hotplate for 24
145 h. Then, 2 ml of HClO₄ (65-71 % w/w) were added to oxidise the organic matter and the
146 residual samples were digested until complete dissolution. 10 mg of Standard Reference

147 Material (SRM) NIST-1648a (urban particulate matter) and 50 mg of certified reference
148 material (CRM) BHVO-2 (basalt) from USGS were processed following the same protocol.
149 The solutions were dried down at 230 °C and then re-fluxed and evaporated twice in 0.3 ml
150 of ca. 16 M HNO₃ to remove the excess of fluorides. The digested solutions were re-fluxed
151 in 300 µl of 7 M HCl and then re-dissolved in 4 ml of 7 M HCl for analysis. HNO₃, HF and
152 HCl purified by sub-boiling distillation in quartz stills and high purity HClO₄ (SpA grade,
153 Romil Ltd) were used.

154 To assess the long-term variability of Zn and Cu isotope signatures in coarse PM at
155 building height, the passive sampler Sigma-2 (Deutscher Wetterdienst) was set up approx. 20
156 m above the street level on the top roof of the Royal School of Mines, Imperial College
157 London. This location is close to roads with high traffic densities (Cromwell Road,
158 Exhibition Road, and Kensington Road). Twelve samples were taken at intervals of approx.
159 five weeks over a period of 18 months between February 2014 and August 2015. The Sigma-
160 2 passive sampler is widely used to monitor continuously atmospheric particles with a size
161 range from 2.5 to 80 µm (PM_{2.5-80}) that are deposited via sedimentation into a small receptor
162 dish that has a diameter of 5.5 cm.³⁵ The dish was acid-cleaned with 4 M HNO₃, 3 M HCl
163 and 2 M distilled HNO₃. The concentrations are given as mass of the elements deposited in
164 the receptor dish per day (ng day⁻¹). The samples were transferred from the receptor dish into
165 PFA vials (Savillex, USA) with 15 ml of 0.1 M HNO₃ and then dried down for subsequent
166 acid digestion. The samples and aliquots of NIST-1648a and BHVO-2 were digested by
167 refluxing in closed vials using a mixture of 3 ml of HNO₃, 1 ml of HF and 0.5 ml of HClO₄
168 over four days on a hot plate at 140 °C. Solutions were evaporated to dryness at 230 °C, re-
169 fluxed in ca. 16 M HNO₃ and 7 M HCl, evaporated again and re-dissolved in 2 ml of 7 M
170 HCl for subsequent analysis.

171 Two samples of Zn ore concentrates from mines in Kazakhstan were purchased from
172 Alex Stewart International to constrain the isotope signature of Zn used for the manufacturing
173 of non-combustion vehicle sources like tires and galvanized steel parts. The samples were
174 ground in an agate pestle and mortar, and digested along with BHVO-2 in duplicate in Teflon
175 vessels in a microwave (Milestone Ethos). Aliquots of 30 mg were digested using a mixture
176 of 6 ml and 2 ml of HNO₃ and HF, respectively, and dried down and re-dissolved in 7 M HCl
177 for subsequent analysis.

178

179 *Determination of element concentrations, enrichment factors and isotope ratios*

180 Samples were prepared in Class 10 laminar flow hoods hosted in metal-free Class 1000 clean
181 laboratories. Dilute acid solutions were prepared using 18.2 MΩ grade water (Millipore
182 system, USA).

183 An aliquot of the digested PM was used for elemental analysis by quadrupole
184 inductively couple plasma mass spectrometry (Q-ICP-MS) using an Agilent 7700x, while the
185 concentrations in the ore concentrates were determined by inductively coupled plasma optical
186 emission spectroscopy (ICP-OES) using a Thermo iCap 6500 Duo. The accuracy of the
187 methods was evaluated by using NIST-1648a and BHVO-2 for all elements used in this study
188 (Cu, Zn, Fe, Al, Sb, Cd) and was within the precision of the certified values.

189 The anthropogenic contribution of Zn, Cu, Fe, Sb and Cd in the PM was assessed
 190 calculating EF using Al as reference element and the upper continental crust as reference
 191 reservoir.³⁶

$$192 \quad EF = \frac{C_{x,s}/C_{Al,s}}{C_{x,c}/C_{Al,c}} \quad [Eq. 1]$$

193 where $C_{x,s}$ and $C_{Al,s}$ represent the concentrations of the element x and Al in the sample,
 194 respectively, and $C_{x,c}$ and $C_{Al,c}$ represent their concentrations in the upper continental crust.
 195 Enrichment factors higher than 5.0 are considered as significant.³⁷

196 Separation of Zn and Cu from the sample matrix prior to isotope analysis was achieved
 197 using anion-exchange chromatography.^{18,38} To this end, 0.7 ml of Bio-Rad AG MP-1 resin
 198 (100–200 mesh) was added to Bio-Rad polypropylene columns with 2 ml of resin reservoir.
 199 The Zn fraction was collected in PFA vials, dried down on a hot plate at 120 °C and treated
 200 with 0.3 ml of ca. 16 M HNO₃ to digest any organic column residue. The solution was dried
 201 again and re-dissolved in 2 ml of 0.1 M HNO₃ for isotopic analysis. The Cu fraction was
 202 dried down, refluxed, re-dissolved in 0.3 ml of 7 M HCl, and further purified using an in-
 203 house made Teflon column of 200 µl of resin reservoir containing 150 µl of the same resin.
 204 Possible effect of isotope fractionation during the ion exchange procedure was addressed by
 205 achieving complete recovery of Cu (96–108%).

206 Isotope ratios of Zn and Cu were determined using a Nu Plasma multi collector ICP-
 207 MS (Nu Instruments Limited, UK) equipped with a Nu DSN-100 Desolvation Nebulizer
 208 System and a glass nebulizer (100 µl min⁻¹). The isotopes ⁶²Ni, ⁶³Cu, ⁶⁴Zn, ⁶⁵Cu, ⁶⁶Zn, ⁶⁷Zn
 209 and ⁶⁸Zn were measured simultaneously and the calculated isotope ratios are referenced to
 210 IRMM-3702 and ERM-AE633 for Zn and Cu, respectively. Isobaric interferences of ⁶⁴Ni
 211 were monitored measuring the intensity of ⁶²Ni but were negligible for all the analysis
 212 performed in this study. All samples were scanned for elements such as Na, Mg, Ca, Ba, etc,
 213 that would cause polyatomic interferences on the plasma.³⁹ The concentrations of the
 214 interfering elements in the fractions were below the detection limit, except for Ca and Fe that
 215 were below 0.36% and 0.25% of the total amount in the sample loaded onto the columns,
 216 respectively, and were not affecting the accuracy of the isotope ratio analysis. Instrumental
 217 mass bias effects were corrected using an in-house ⁶⁴Zn–⁶⁷Zn double-spike for Zn and
 218 standard sample bracketing for Cu.^{40, 41} Further analytical details of the anion-exchange
 219 procedure, spike calibration and mass bias corrections are given in the Supporting
 220 Information. The Zn and Cu isotope ratios are reported as $\delta^{66}\text{Zn}_{\text{IRMM}}$ and $\delta^{66}\text{Cu}_{\text{AE633}}$
 221 according to Eq. 2 and Eq. 3:

$$222 \quad \delta^{66}\text{Zn}_{\text{IRMM}} = \left[\frac{({}^{66}\text{Zn}/{}^{64}\text{Zn})_{\text{sample}}}{({}^{66}\text{Zn}/{}^{64}\text{Zn})_{\text{IRMM}}} - 1 \right] \times 1000 \quad [Eq. 2]$$

$$223 \quad \delta^{65}\text{Cu}_{\text{AE633}} = \left[\frac{({}^{65}\text{Cu}/{}^{63}\text{Cu})_{\text{sample}}}{({}^{65}\text{Cu}/{}^{63}\text{Cu})_{\text{AE633}}} - 1 \right] \times 1000 \quad [Eq. 3]$$

224 Previously published Zn and Cu isotope ratios referring to JMC 3-0749L Lyon and NIST 976
 225 standards were recalculated to IRMM-3702 and SRM AE633 using an isotopic offset of
 226 +0.32‰ for Zn and no isotopic offset for Cu.^{11, 42} The analytical precision of the isotope

227 analysis of individual samples (2SD) has been assessed using one passage of the digested
228 sample and at least three individual sample measurements. Accuracy and reproducibility
229 were assessed for each analytical session by repeated measurements of BHVO-2 and
230 commercial single element solutions (denoted as Romil Zn and Romil Cu). The isotopic
231 composition for BHVO-2 ($\delta^{66}\text{Zn}_{\text{IRMM}} = +0.11 \pm 0.25\%$, $n=5$), Romil Zn ($-9.10 \pm 0.10\%$, $n=4$)
232 and Romil Cu ($\delta^{65}\text{Cu}_{\text{AE633}} = +0.18 \pm 0.05\%$, $n=4$) are in good agreement with previous
233 published data.⁴² Average isotopic compositions of NIST-1648a determined from individual
234 analytical sessions over six months were $\delta^{66}\text{Zn}_{\text{IRMM}} = -0.19 \pm 0.15\%$ ($n=6$) and $\delta^{65}\text{Cu}_{\text{AE633}} =$
235 $+0.11 \pm 0.20\%$ ($n=6$).

236

237 3. Results and Discussion

238

239 3.1. Spatial and temporal variability of concentrations, enrichment factors and isotope 240 ratios in PM_{10} in Barcelona

241

242 Table 1 shows concentrations (Zn, Cu, Fe, Sb and Cd), EF (EF_{Zn} , EF_{Cu} , EF_{Fe} , EF_{Sb} and EF_{Cd}),
243 and isotope signatures ($\delta^{66}\text{Zn}_{\text{IRMM}}$ and $\delta^{65}\text{Cu}_{\text{AE633}}$) determined in PM_{10} collected in Barcelona
244 at sites with low (Torre Girona and Palau Reial) and high (Corsega Avenue and Valencia
245 Avenue) traffic occurrence during 2012 and 2013.

246 The concentrations of Cu, Fe and Sb are higher at the sites with high traffic (T1–T10)
247 than at the sites with low traffic (B1–B10). During February and March 2012, the
248 concentrations of Cu ($76 \pm 31 \text{ ng m}^{-3}$), Fe ($1543 \pm 631 \text{ ng m}^{-3}$) and Sb ($8 \pm 4 \text{ ng m}^{-3}$) in the PM_{10}
249 collected at Corsega Avenue are significantly higher than those measured at the low traffic
250 site in Torre Girona (Table 1). The concentrations of Zn and Cd, in contrast, are similar at
251 both sites. The sampling campaign during June 2013 shows higher concentrations of Cu
252 ($53 \pm 15 \text{ ng m}^{-3}$), Fe ($1140 \pm 317 \text{ ng m}^{-3}$) and Sb ($6 \pm 3 \text{ ng m}^{-3}$) at Valencia Avenue compared to
253 Palau Reial (low traffic site). The concentrations of all the elements are higher in autumn
254 2012 than in spring 2013, possibly reflecting drier weather conditions leading to decreased
255 deposition.⁴³

256 We find large enrichments of Cu, Fe and Sb, which reflect significant anthropogenic
257 contribution (Figure S4). The EF are higher at Valencia Avenue ($\text{EF}_{\text{Fe}} = 5.7 \pm 0.6$, $\text{EF}_{\text{Cu}} =$
258 268 ± 26 and $\text{EF}_{\text{Sb}} = 8678 \pm 596$) and Corsega Avenue ($\text{EF}_{\text{Fe}} = 3.1 \pm 0.9$, $\text{EF}_{\text{Cu}} = 155 \pm 47$ and
259 $\text{EF}_{\text{Sb}} = 4282 \pm 1239$) than at Palau Reial and Torre Girona (Table 1), respectively. The EF_{Zn}
260 and EF_{Cd} , in contrast, are similar at the low and high traffic sites. The EF_{Zn} ranges between
261 77 and 180 and between 172 and 347 during 2012 and 2013, respectively. The EF_{Cd} ranges
262 between 67 and 381, except in sample T6, and between 132 and 312 during 2012 and 2013,
263 respectively (Table 1). The EF_{Zn} , EF_{Cu} and EF_{Sb} in Valencia Avenue are significantly higher
264 than those in Corsega Avenue which averages 3000 vehicles day^{-1} less.

265 The isotope ratios of Zn and Cu are shown in Figure 1. Zinc is isotopically light with
266 $\delta^{66}\text{Zn}_{\text{IRMM}}$ ranging between -0.13 ± 0.09 and $-0.51 \pm 0.05\%$ (Table 1). The temporal (between
267 sampling campaigns) and spatial (between sites) variability are significant relative to the

268 typical average internal precision of 0.07‰ for each isotope ratio measurement. Isotopic
269 light Zn found in PM₁₀ and emissions from high temperature industrial activities^{15, 16} are in
270 line with our results suggesting important contribution from metallurgical processes in PM in
271 Barcelona.^{32, 33} The insignificant correlations between $\delta^{66}\text{Zn}_{\text{IRMM}}$ and EF_{Zn} and EF_{Sb} (Figure
272 2a and 2b), and the weak correlation between EF_{Zn} and Sb and Fe which are well established
273 tracers for brake wear particles (Figure 3a) support this hypothesis. Furthermore, samples
274 with negative isotope signatures at Torre Girona and Palau Reial, i.e., the sites located close
275 to the metallurgical industry in Barcelona, are also enriched in Zn and Cd (Figure S4).

276 The spatial and temporal variations of $\delta^{65}\text{Cu}_{\text{AE633}}$ range between $+0.04\pm 0.20$ and
277 $+0.33\pm 0.15\%$ (Table 1), with one negative value measured in sample B3 ($\delta^{65}\text{Cu}_{\text{AE633}} =$
278 $-0.43\pm 0.10\%$). Significant correlations between $\delta^{65}\text{Cu}_{\text{AE633}}$ and EF_{Cu} and EF_{Sb} (Figures 2d
279 and 2e) suggest that the observed Cu isotope signature is controlled by non-exhaust vehicle
280 emissions, i.e., brake wear.⁴⁴ This is indeed supported by the strong positive correlation
281 between the EF_{Cu} and EF_{Fe} ($R^2 = 0.9722$) and the EF_{Cu} and EF_{Sb} ($R^2 = 0.9305$) (Figure 3b).
282 Consequently, an estimated Cu isotope signature for brake-derived particles of $\delta^{65}\text{Cu}_{\text{AE633}} =$
283 $+0.18\pm 0.14\%$ ($n=19$, except B3) can be proposed using the average isotopic composition of
284 the PM₁₀. This is in line with the $\delta^{65}\text{Cu}_{\text{AE633}}$ determined for primary Cu sulphides ranging
285 between -1 and $+1\%$,²² and Cu sulphides being the dominant chemical species in brake
286 lining materials.^{44, 45} Sample B3 has a very light Cu isotope signature along with a low EF_{Cu}
287 ($\text{EF}_{\text{Cu}} = 43$) and EF_{Sb} ($\text{EF}_{\text{Sb}} = 1327$) (Figures 2d and 2e). This light signature may be
288 explained by the temporal contribution from flue gas emissions from the metallurgical
289 industry, which in fact has been previously proposed to explain the enrichment of Cu in PM
290 in Barcelona.^{32, 33}

291

292 3.2. Spatial and temporal variability of concentrations, enrichment factors and isotope 293 ratios in PM_{2.5-80} in London

294

295 Table 1 shows concentrations (Zn, Cu, Fe, Sb and Cd), EF (EF_{Zn} , EF_{Cu} , EF_{Fe} , EF_{Sb} and EF_{Cd}),
296 and isotope signatures ($\delta^{66}\text{Zn}_{\text{IRMM}}$ and $\delta^{65}\text{Cu}_{\text{AE633}}$) determined in PM collected using a
297 passive sampler in London.

298 Elemental concentrations and EF were low during February 2014 (sample S1) and
299 between November 2014 and February 2015 (samples S7, S8 and S9). This is likely because
300 of high wet depositional flux of particles during periods of rain associated with the winter
301 season in London.⁴⁶

302 The $\delta^{66}\text{Zn}_{\text{IRMM}}$ values vary between $+0.03\pm 0.04$ and $+0.49\pm 0.02\%$ (Table 1) and
303 correlate positively with the EF_{Zn} , except sample S5 which was collected between September
304 and October 2014 (Figure 2a). The different $\delta^{66}\text{Zn}_{\text{IRMM}}$ and significantly high EF_{Zn} and EF_{Cd}
305 for sample S5 (Table 1) indicate additional sources. The $\delta^{66}\text{Zn}_{\text{IRMM}}$ values are weakly
306 correlated with EF_{Sb} (Figure 2c), suggesting some contribution from brake wear. The samples
307 S6, S7, S9 and S12 have the highest EF_{Zn} and $\delta^{66}\text{Zn}_{\text{IRMM}}$ values close to 0.00‰. The
308 $\delta^{66}\text{Zn}_{\text{IRMM}}$ in the PM enriched in Zn agree well with those found for ZnO which is added to

309 tire-tread rubber to facilitate the vulcanization process,¹⁴ and with ore concentrates (mainly
310 sphalerite) analysed in our study ($\delta^{66}\text{Zn}_{\text{IRMM}} = +0.03 \pm 0.10\%$, two samples). Particles from
311 tire wear are in general larger than $10 \mu\text{m}$,^{44,45} and therefore have possibly been preferentially
312 accumulated in the passive sampler, supporting further contribution from tire wear.

313 The $\delta^{65}\text{Cu}_{\text{AE633}}$ values vary between $+0.37 \pm 0.17$ to $+0.97 \pm 0.21\%$ (Table 1). These
314 values are significantly heavier than in PM_{10} collected in Barcelona. We find significant
315 isotope variability over the entire time period assessed, but most notable are the heavier
316 $\delta^{65}\text{Cu}_{\text{AE633}}$ signatures found in samples S6, S7, S8 and S9 collected during winter and end of
317 autumn (Figure 1b). This could suggest that emissions from fossil fuel combustion control
318 significantly the isotope signatures, with a maximum peak on $\delta^{65}\text{Cu}_{\text{AE633}}$ during November
319 and December 2014 (S7). The Cu/Sb ratio of brake wear is typically 4.6 ± 2.3 .^{47,54} The Cu/Sb
320 ratios in PM collected during winter in London (Table 1) are well above this value which
321 supports an important contribution from fuel or oil combustion.

322

323 **3.3. Conceptual models for the controls of Zn and Cu isotope fingerprints in particulate** 324 **matter in Barcelona and London**

325

326 Figure 4 shows preliminary conceptual models summarizing the possible controls of Zn and
327 Cu isotope signatures in fine and large PM collected in Barcelona and London, respectively.
328 These models warrant further work; however, they form an important starting point for the
329 possible inclusion of these isotope systems in air quality studies.

330 In Barcelona, we propose that the isotope signatures identify significant contributions
331 from emissions from metallurgical and non-exhaust vehicle emissions for Zn and Cu in PM_{10} ,
332 respectively. The influence of emissions from metallurgy for Zn is supported by (i) the lack
333 of correlation between $\delta^{66}\text{Zn}_{\text{IRMM}}$ and the EF_{Sb} (Figure 2b), and between the EF_{Zn} , EF_{Sb} and
334 EF_{Fe} (Figure 3); (ii) the high variability in the $\delta^{66}\text{Zn}_{\text{IRMM}}$ at the low and high traffic sites, and
335 the similarity in the EF_{Cd} and EF_{Zn} in both sites (Figure 1a and Table 1); and (iii) the known
336 light isotope signature of Zn in PM emitted from metallurgical and coal combustion
337 processes.¹⁵⁻¹⁷ Significant contribution from brake wear to Cu enrichment in PM_{10} is
338 supported by (i) the correlation between the EF_{Cu} , EF_{Fe} and EF_{Sb} , which are typical tracers of
339 brake wear (Figure 3), and (ii) the Cu/Sb ratios in the PM_{10} (Table 1) which are close to the
340 Cu/Sb ratios previously reported for brake wear particles.^{47,54}

341 In London, we propose that Zn and Cu in $\text{PM}_{2.5-80}$ are dominated by non-exhaust
342 emissions from road vehicles. The correlation between $\delta^{66}\text{Zn}_{\text{IRMM}}$ and EF_{Sb} (Figure 2c), and
343 the similarity between $\delta^{66}\text{Zn}_{\text{IRMM}}$ of the $\text{PM}_{2.5-80}$ samples enriched in Zn (Table 1) and of ore
344 minerals typically used in the production of tires and galvanized steel¹²⁻¹⁴ support this idea.
345 The $\delta^{65}\text{Cu}_{\text{AE633}}$ in the $\text{PM}_{2.5-80}$ collected during winter and late autumn is heavier than during
346 the other seasons, and we propose that this is due to the dominant contribution of isotopically
347 heavy Cu in residual particles from fossil fuel combustion, as previously found for Zn in PM
348 from smelting and coal combustion.^{13, 16, 17} The Cu/Sb ratios of $\text{PM}_{2.5-80}$ ($\text{Cu/Sb} = 19 \pm 7$) are
349 significantly higher than those typically found in brakes ($\text{Cu/Sb} = 4.6 \pm 2.3$)^{47,54} and those of

350 PM₁₀ collected in Barcelona (Cu/Sb=9±2) (Table 1). The $\delta^{65}\text{Cu}_{\text{AE633}}$ and the Cu/Sb ratios of
351 PM_{2.5-80} collected during spring and summer in London are closer to those of PM₁₀ in
352 Barcelona (Table 1 and Figure 4). These conclusions are in line with the strong correlation
353 between the $\delta^{65}\text{Cu}_{\text{AE633}}$ and the Cu/Sb ratios ($R^2 = 0.820$) in the PM (Figure 2f), the
354 significantly isotopic heavier Cu found in London compared to Barcelona, and the
355 contribution of brake wear particles in Barcelona which are typically smaller than 10 μm .^{48, 49}
356

357 **3.4. Zinc and Cu isotope signatures in atmospheric particulate matter: a global** 358 **perspective** 359

360 Figure 5 shows Zn and Cu isotope signatures determined in atmospheric PM collected from
361 cities in Europe and South America (Barcelona, London, Metz and São Paulo)^{19, 20} and over
362 the North Atlantic Ocean.^{18, 21} In an attempt to characterise potential isotope signatures of
363 natural and anthropogenic sources, we also plot the measured isotope ratios of various
364 different source materials.

365 With respect to Zn, we constrain the isotope signature of natural sources (wind-blown
366 mineral dust and soil) using values determined for igneous rocks.¹¹ The anthropogenic
367 signatures include (i) ore concentrates and sphalerite¹²⁻¹⁴ representing non-exhaust traffic
368 sources (i.e., tire wear, galvanised steel), and (ii) PM collected around smelters and from
369 coal-fired power plants representing PM from high temperature processes.^{15, 17, 20} As shown
370 in Figure 5, we find that the isotopic compositions of Zn in PM collected over the North
371 Atlantic region overlap mostly with those in ore concentrates and minerals.^{11-14, 18, 21} This
372 suggests that either natural sources from wind-blown mineral dust or anthropogenic sources
373 derived from non-exhaust traffic emissions are dominant. Isotopically light Zn is dominant in
374 most PM collected in São Paulo and Barcelona,²⁰ and we propose that this reflects a possible
375 control of Zn from high temperature processes. This is supported by previous work that
376 shows that trace element concentrations in PM in Barcelona and São Paulo are affected by
377 metallurgical emissions and biomass burning, respectively.^{22, 32, 33} The isotope signatures in
378 PM collected in Metz and in time series in London are in good agreement with the isotopic
379 composition of sphalerite, i.e., non-exhaust traffic emissions.

380 With respect to Cu, the isotope signatures in PM collected in Barcelona and over the
381 North Atlantic region overlap with the signature for primary Cu sulphides ($\delta^{65}\text{Cu}_{\text{AE633}} = -1$ to
382 $+1\text{‰}$).^{18, 21, 22} The Cu signatures in PM_{2.5-80} collected in London are significantly different
383 from the $\delta^{65}\text{Cu}_{\text{AE633}}$ in natural dust, most probably due to the influence of combustion
384 emissions during the winter season.^{13, 16, 17}

385 Figure 5 suggests that the cities investigated so far have their own ‘isotope signature’
386 and we propose that the isotope fingerprints reflect the importance of emissions from high
387 temperature processes and non-exhaust traffic emissions such as brake and tire wear. These
388 observations are among the first to place constraints on the use of Zn and Cu isotopes as
389 tracers of anthropogenic sources in atmospheric PM and support previous hypothesis
390 suggesting that smelting and combustion induce a significant isotope fractionation.
391

392 **Acknowledgements**

393 R.O.G. thanks The European Commission (FP7-PEOPLE-2012-IEF) for funding the project
394 ISOTRACE (proposal 329878). The authors wish to thank the MAGIC group and in
395 particular Katharina Kreissig at Imperial College for their assistance in the laboratories,
396 Emma Humphreys-Williams (Natural History Museum) for conducting the ICP-OES
397 analysis, and the important feedback provided by three reviewers. Fraser Wigley is thanked
398 for his help during the collection of samples in London.

399

400 **Supporting Information**

401 Further details regarding the sampling locations in Barcelona, ion exchange procedure, mass
402 bias correction for Zn isotope analysis and analytical data are detailed in the Supporting
403 information. This information is available free of charge via the Internet at
404 <http://pubs.acs.org/>.

Table 1. Concentrations, EF and isotope signatures in PM collected in Barcelona (PM₁₀) and London (PM_{2.5-80}).*: sample S5 has not been considered tocalculate the average EF_{Cd}.

	Sample label	Date of collection	Concentrations ng m ⁻³ (Barcelona) and ng day ⁻¹ (London)							EF _{Zn}	EF _{Cu}	EF _{Fe}	EF _{Sb}	EF _{Cd}	$\delta^{66}\text{Zn}_{\text{HRMM}}$ (‰)	±2SD	$\delta^{65}\text{Cu}_{\text{AE633}}$ (‰)	±2SD	
			Al	Zn	Cu	Fe	Sb	Cd	Cu/Sb										
Barcelona (PM ₁₀)	B1	02/2012	1549	102	93	2114	10.6	0.31	8.8	77	90	2.0	2824	81	-0.29	0.05	+0.20	0.02	
	B2	02/2012	874	102	38	866	5.0	0.21	7.7	137	66	1.5	2347	101	-0.40	0.05	+0.15	0.06	
	B3	03/2012	694	62	20	575	2.2	0.17	9.0	105	43	1.2	1327	100	-0.16	0.05	-0.43	0.10	
	Torre Girona	B4	03/2012	774	101	51	1208	6.5	0.38	7.8	153	98	2.3	3460	204	-0.44	0.05	+0.20	0.05
	B5	03/2012	534	36	13	384	1.9	0.09	6.9	78	38	1.1	1498	67	-0.28	0.05	+0.04	0.05	
	B6	03/2012	574	87	36	763	3.7	0.53	9.7	179	93	1.9	2642	381	-0.24	0.07	+0.15	0.03	
	Average±SD		833±373	82±28	42±29	985±620	5±4	0.3±0.2		122±42	71±27	1.7±0.5	2350±815	156±121					
Corsega Avenue	T1	02/2012	992	125	128	2658	12.9	0.33	9.9	148	192	3.9	5358	139	-0.30	0.06	+0.23	0.02	
	T2	02/2012	601	92	77	1481	7.8	0.22	10.0	180	193	3.6	5315	152	-0.22	0.11	+0.20	0.05	
	T3	03/2012	809	73	51	1186	6.0	0.18	8.4	106	93	2.1	3041	94	-0.24	0.15	+0.33	0.15	
	T4	03/2012	556	51	40	773	3.4	0.18	11.6	108	107	2.0	2533	130	-0.37	0.09	+0.25	0.05	
	T5	03/2012	807	115	80	1668	8.3	0.41	9.7	167	149	3.0	4242	210	-0.25	0.05	+0.22	0.04	
	T6	03/2012	594	78	78	1490	7.5	0.96	10.4	155	196	3.7	5200	663	-0.44	0.09	+0.22	0.03	
	Average±SD		727±171	89±28	76±31	1543±631	8±4	0.4±0.3		144±31	155±47	3.1±0.9	4282±1239	231±215					
Palau Reial	B7	06/2013	278	56	26	597	3.3	0.21	7.8	238	138	3.1	4856	312	-0.16	0.05	+0.26	0.11	
	B8	06/2013	184	48	16	406	1.9	0.12	8.1	304	129	3.2	4351	262	-0.13	0.09	+0.04	0.05	
	B9	06/2013	282	83	33	754	3.9	0.15	8.3	347	174	3.9	5751	216	-0.28	0.04	+0.04	0.21	
	B10	06/2013	302	44	26	674	3.9	0.10	6.7	172	130	3.3	5324	132	-0.51	0.05	+0.13	0.17	
	Average±SD		262±53	58±18	25±7	608±149	3±1	0.15±0.05		265±77	143±22	3.4±0.4	5071±603	231±77					
Valencia Avenue	T7	06/2013	386	91	62	1313	8.2	0.26	7.6	278	242	5.0	8753	273	-0.36	0.06	+0.11	0.09	
	T8	06/2013	344	80	63	1358	7.8	0.17	8.0	274	274	5.8	9375	199	-0.39	0.07	+0.09	0.08	
	T9	06/2013	321	76	54	1217	6.2	0.14	8.8	280	254	5.6	7922	178	-0.23	0.06	+0.24	0.06	
	T10	06/2013	154	40	31	673	3.3	0.05	9.5	307	300	6.4	8661	132	-0.27	0.05	+0.24	0.04	
	Average±SD		301±102	72±23	53±15	1140±317	6±3	0.16±0.09		285±15	268±26	5.7±0.6	8678±596	196±59					
London (PM _{2.5-80})	S1	02/2014–03/2014	406	43	14	323	0.7	0.02	20	123	51	1.2	704	25	+0.32	0.12	+0.58	0.15	
	S2	03/2014–05/2014	746	66	21	827	1.3	0.06	16	104	43	1.6	723	34	+0.37	0.10	+0.37	0.17	
	S3	07/2014–08/2014	496	61	13	504	1.1	0.04	12	147	39	1.5	891	32	+0.34	0.04	+0.55	0.15	
	S4	08/2014–09/2014	580	59	18	557	1.3	0.06	14	120	47	1.5	886	40	+0.49	0.02	+0.46	0.12	
	S5	09/2014–10/2014	314	61	18	283	0.6	0.21	32	239	87	1.3	729	271	+0.37	0.20	+0.51	0.20	
	S6	10/2014–11/2014	352	56	22	493	0.7	0.05	31	188	91	2.1	810	58	+0.16	0.16	+0.88	0.22	
	S7	11/2014–12/2014	207	35	11	265	0.5	0.02	24	197	78	1.9	896	33	+0.08	0.05	+0.97	0.21	
	S8	12/2014–01/2015	281	32	14	300	0.6	0.02	22	132	72	1.6	902	30	+0.19	0.17	+0.84	0.21	
	S9	01/2015–02/2015	282	43	14	382	0.7	0.03	19	180	74	2.0	1077	37	+0.14	0.04	+0.66	0.17	
	S10	03/2015–04/2015	660	67	18	822	1.5	0.04	13	119	42	1.8	906	23	+0.12	0.09	+0.52	0.14	
	S11	05/2015–06/2015	670	81	20	787	1.8	0.05	12	143	45	1.7	1077	31	+0.14	0.13	+0.52	0.22	
	S12	07/2015–08/2015	478	65	18	520	1.2	0.04	14	160	55	1.6	1053	34	+0.03	0.04	+0.53	0.11	
	Average±SD		456±178	56±15	17±4	505±210	1.0±0.5	0.05±0.05		154±40	60±19	1.7±0.3	888±132	34±10*					

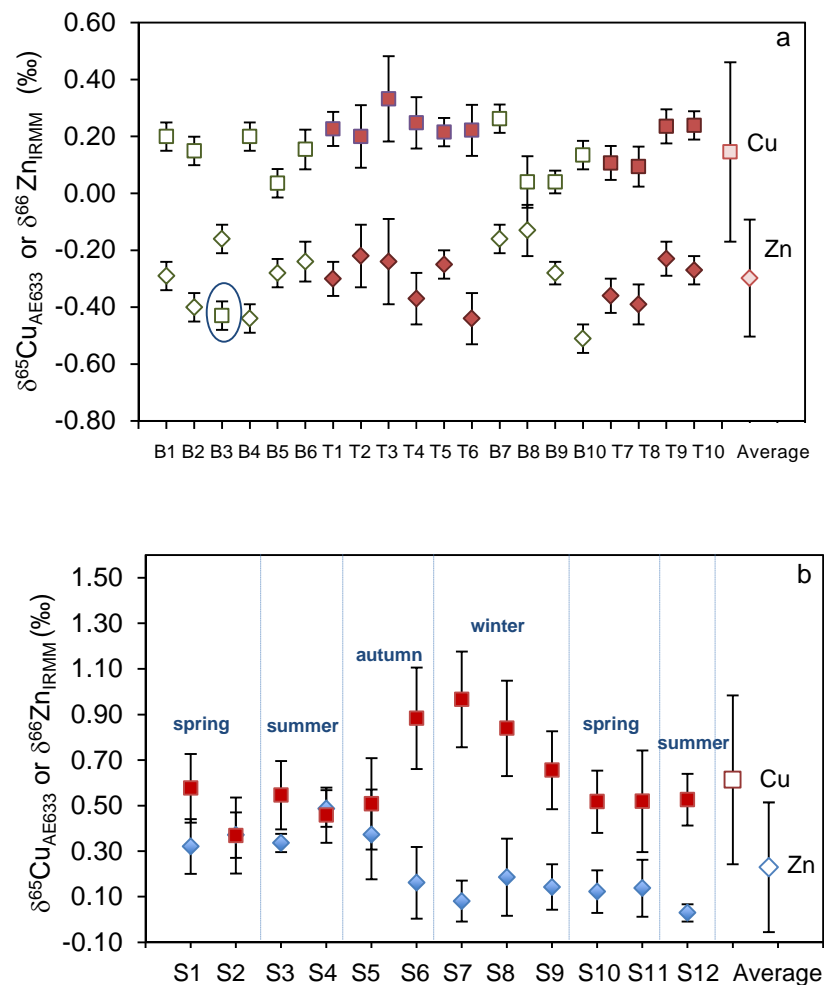


Figure 1. a) Variability in the Zn (diamonds) and Cu (squares) isotope signatures (expressed as $\delta^{66}\text{Zn}_{\text{IRMM}}$ and $\delta^{65}\text{Cu}_{\text{AE633}}$, respectively) in PM collected in Barcelona at Torre Girona (B1–B6) and Corsega (T1–T6) during autumn 2012, and at Palau Reial (B7–B10) and Valencia (T7–T10) during spring 2013. Open and closed symbols represent low traffic and high traffic sites, respectively. The sample B3 is circled as it shows an anomalous value for $\delta^{65}\text{Cu}_{\text{AE633}}$. b) Zinc and Cu isotope variability in PM collected between February 2014 and August 2015 in London. Average Zn and Cu isotopic compositions are also shown in the figures. Error bars represent the 2σ standard deviation of repeated sample measurements ($n \geq 3$).

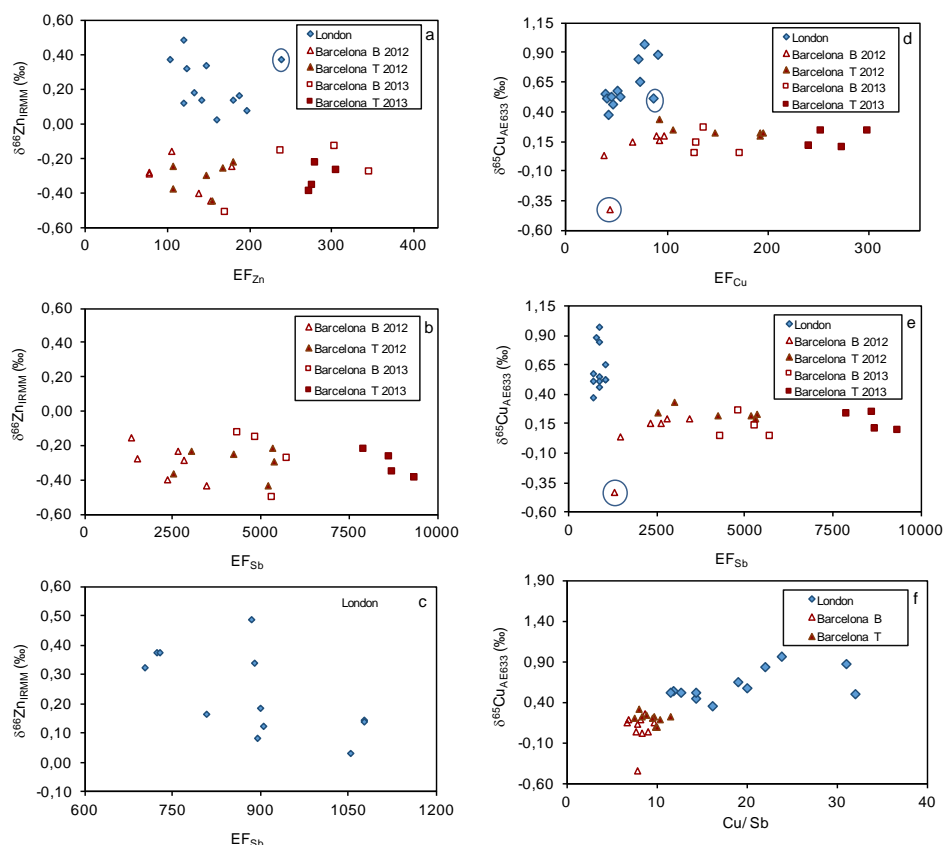


Figure 2. a) Zinc isotope composition vs. the EF of Zn (EF_{Zn}). The anomalous value for S5 in London (circled) is discussed in the text. b) and c) Zinc isotope compositions for PM collected in Barcelona and London, respectively, plotted vs. EF_{Sb} . d) Copper isotope compositions vs. EF_{Cu} in PM analysed during this study. Samples S5 and B3 are circled, as they do not follow the general trends. e) Copper isotope compositions plotted against EF_{Sb} . Sample B3 is circled and discussed in the text. f) Copper isotope compositions vs. Cu/Sb ratios. Open and closed symbols represent low traffic (B) and high traffic (T) sites, respectively.

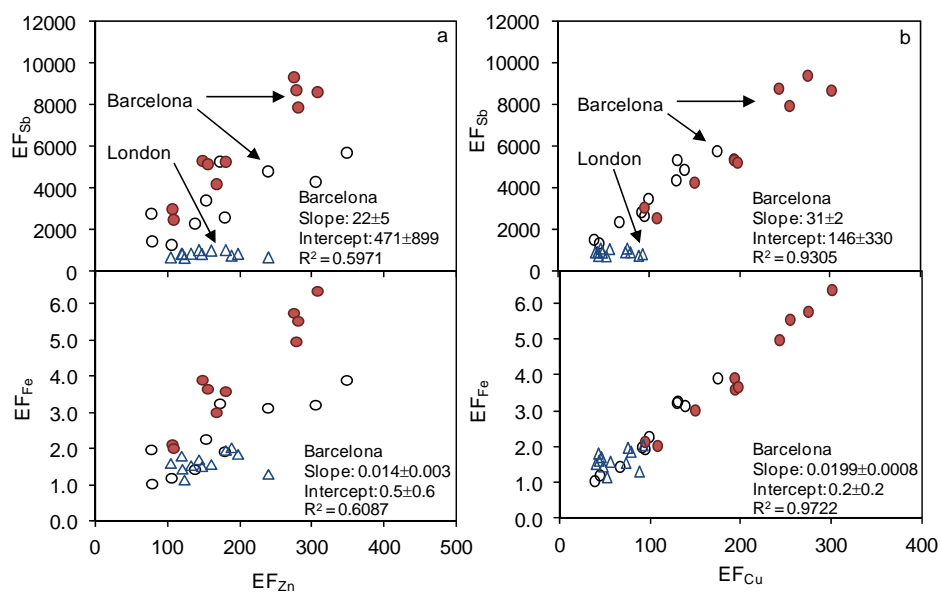


Figure 3. Relationship between the EF of Zn, Sb and Fe (panel a) and the EF of Cu, Sb and Fe (panel b) in PM collected in Barcelona (circles) and London (triangles). Open and closed circles represent low traffic and high traffic sites in Barcelona, respectively. The slopes ($\pm 1SD$), intercepts ($\pm 1SD$) and R^2 of the regression lines for PM collected in Barcelona are given in the panels.

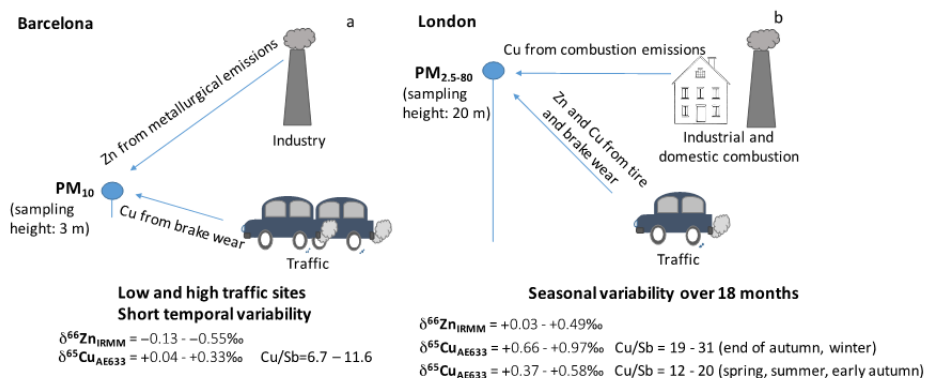


Figure 4. Proposed conceptual model of possible controls of Zn and Cu isotope signatures in fine PM in Barcelona (panel a) and coarse PM in London (panel b) derived from this study. In Barcelona, Zn and Cu are dominated by emissions from metallurgical industries and from non-exhaust vehicle emissions (brake wear), respectively. In London, Zn and Cu are both largely dominated by emissions from non-exhaust vehicle sources, unless during winter, where the heavy $\delta^{65}\text{Cu}_{\text{AE633}}$ suggests an increased contribution from fossil fuel combustion.

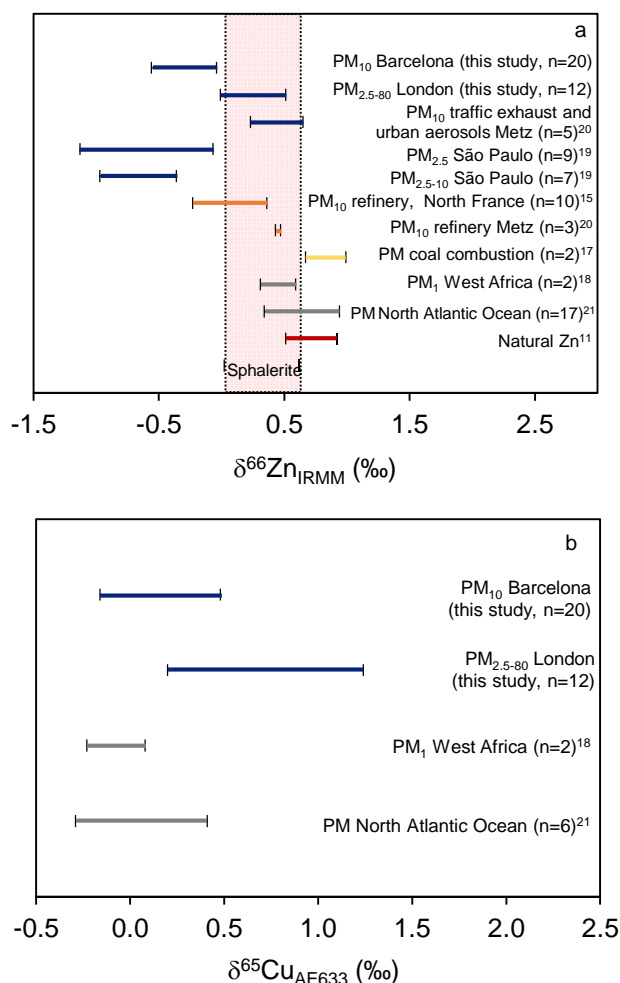


Figure 5. Zinc (panel a) and Cu (panel b) isotope compositions in PM collected at different locations around the world. The range of $\delta^{66}\text{Zn}_{\text{IRMM}}$ determined for sphalerite and ore concentrates (literature and this study) is shown using the shaded area.¹²⁻¹⁴ The $\delta^{66}\text{Zn}_{\text{IRMM}}$ in rocks ranges between +0.52 and +0.92‰ (panel a), and the $\delta^{65}\text{Cu}_{\text{AE633}}$ in Cu sulphides ranges between -1 and +1‰.^{11,22} The $\delta^{66}\text{Zn}_{\text{Lyon}}$ and $\delta^{65}\text{Cu}_{\text{NIST976}}$ taken from the literature were normalised to $\delta^{66}\text{Zn}_{\text{IRMM}}$ and $\delta^{65}\text{Cu}_{\text{AE633}}$, respectively, assuming an isotope offset of $\Delta^{66}\text{Zn}_{\text{IRMM-Lyon}} = +0.32\text{‰}$ and no isotope offset for Cu ($\Delta^{65}\text{Cu}_{\text{NIST976-AE633}} \approx -0.01 \pm 0.04\text{‰}$).^{11, 42} Data obtained during this study and other cities in Europe and South America are presented in blue color whereas data from literature for PM from smelters and coal-fired power plants is shown in orange and yellow, respectively. Additional data for natural PM and natural sources of Zn are presented in grey and red, respectively.

References

1. Tositti, L.; Brattich, E.; Masiol, M.; Baldacci, D.; Ceccato, D.; Parmeggiani, S.; Stracquadanio, M.; Zappoli, S., Source apportionment of particulate matter in a large city of southeastern Po Valley (Bologna, Italy). *Environ Sci Pollut Res* **2014**, *21*, (2), 872-890.
2. Dutton, S. J.; Vedal, S.; Piedrahita, R.; Milford, J. B.; Miller, S. L.; Hannigan, M. P., Source Apportionment Using Positive Matrix Factorization on Daily Measurements of Inorganic and Organic Speciated PM(2.5). *Atmospheric environment (Oxford, England : 1994)* **2010**, *44*, (23), 2731-2741.
3. Wiederhold, J. G., Metal Stable Isotope Signatures as Tracers in Environmental Geochemistry. *Environmental Science & Technology* **2015**, *49*, (5), 2606-2624.
4. Song, X.-H.; Polissar, A. V.; Hopke, P. K., Sources of fine particle composition in the northeastern US. *Atmospheric Environment* **2001**, *35*, (31), 5277-5286.
5. Al-Masri, M. S.; Al-Kharfan, K.; Al-Shamali, K., Speciation of Pb, Cu and Zn determined by sequential extraction for identification of air pollution sources in Syria. *Atmospheric Environment* **2006**, *40*, (4), 753-761.
6. Councill, T. B.; Duckenfield, K. U.; Landa, E. R.; Callender, E., Tire-Wear Particles as a Source of Zinc to the Environment. *Environmental Science & Technology* **2004**, *38*, (15), 4206-4214.
7. Batonneau, Y.; Bremard, C.; Gengembre, L.; Laureyns, J.; Le Maguer, A.; Le Maguer, D.; Perdrix, E.; Sobanska, S., Speciation of PM10 Sources of Airborne Nonferrous Metals within the 3-km Zone of Lead/Zinc Smelters. *Environmental Science & Technology* **2004**, *38*, (20), 5281-5289.
8. Wang, X.; Sato, T.; Xing, B.; Tamamura, S.; Tao, S., Source identification, size distribution and indicator screening of airborne trace metals in Kanazawa, Japan. *Journal of Aerosol Science* **2005**, *36*, (2), 197-210.
9. Al-Momani, I. F.; Daradkeh, A. S.; Haj-Hussein, A. T.; Yousef, Y. A.; Jaradat, Q. M.; Momani, K. A., Trace elements in daily collected aerosols in Al-Hashimya, central Jordan. *Atmospheric Research* **2005**, *73*, (1-2), 87-100.
10. Fernández, A. J.; Ternero, M.; Barragán, F. J.; Jiménez, J. C., An approach to characterization of sources of urban airborne particles through heavy metal speciation. *Chemosphere - Global Change Science* **2000**, *2*, (2), 123-136.
11. Cloquet, C.; Carignan, J.; Lehmann, M.; Vanhaecke, F., Variation in the isotopic composition of zinc in the natural environment and the use of zinc isotopes in biogeosciences: a review. *Analytical and bioanalytical chemistry* **2008**, *390*, (2), 451-463.
12. John, S. G.; Genevieve Park, J.; Zhang, Z.; Boyle, E. A., The isotopic composition of some common forms of anthropogenic zinc. *Chemical Geology* **2007**, *245*, (1-2), 61-69.
13. Sivry, Y.; Riotte, J.; Sonke, J. E.; Audry, S.; Schäfer, J.; Viers, J.; Blanc, G.; Freydier, R.; Dupré, B., Zn isotopes as tracers of anthropogenic pollution from Zn-ore smelters The Riou Mort-Lot River system. *Chemical Geology* **2008**, *255*, (3-4), 295-304.
14. Sonke, J. E.; Sivry, Y.; Viers, J.; Freydier, R.; Dejonghe, L.; André, L.; Aggarwal, J. K.; Fontan, F.; Dupré, B., Historical variations in the isotopic composition of atmospheric zinc deposition from a zinc smelter. *Chemical Geology* **2008**, *252*, (3-4), 145-157.
15. Mattielli, N.; Petit, J. C. J.; Deboudt, K.; Flament, P.; Perdrix, E.; Taillez, A.; Rimetz-Planchon, J.; Weis, D., Zn isotope study of atmospheric emissions and dry

- depositions within a 5 km radius of a Pb–Zn refinery. *Atmospheric Environment* **2009**, *43*, (6), 1265-1272.
16. Ochoa González, R.; Weiss, D. J., Zinc isotope variability in three coal-fired power plants: A predictive model for determining isotopic fractionation during combustion. *Environmental Science & Technology* **2015**.
17. Borrok, D. M.; Gieré, R.; Ren, M.; Landa, E. R., Zinc Isotopic Composition of Particulate Matter Generated during the Combustion of Coal and Coal + Tire-Derived Fuels. *Environmental Science & Technology* **2010**, *44*, (23), 9219-9224.
18. Dong, S.; Weiss, D. J.; Strekopytov, S.; Kreissig, K.; Sun, Y.; Baker, A. R.; Formenti, P., Stable isotope ratio measurements of Cu and Zn in mineral dust (bulk and size fractions) from the Taklimakan Desert and the Sahel and in aerosols from the eastern tropical North Atlantic Ocean. *Talanta* **2013**, *114*, 103-109.
19. Gioia, S.; Weiss, D.; Coles, B.; Arnold, T.; Babinski, M., Accurate and Precise Zinc Isotope Ratio Measurements in Urban Aerosols. *Analytical Chemistry* **2008**, *80*, (24), 9776-9780.
20. Cloquet, C.; Carignan, J.; Libourel, G., Isotopic Composition of Zn and Pb Atmospheric Depositions in an Urban/Periurban Area of Northeastern France. *Environmental Science & Technology* **2006**, *40*, (21), 6594-6600.
21. Little, S. H.; Vance, D.; Walker-Brown, C.; Landing, W. M., The oceanic mass balance of copper and zinc isotopes, investigated by analysis of their inputs, and outputs to ferromanganese oxide sediments. *Geochimica et Cosmochimica Acta* **2014**, *125*, 673-693.
22. Kimball, B. E.; Mathur, R.; Dohnalkova, A. C.; Wall, A. J.; Runkel, R. L.; Brantley, S. L., Copper isotope fractionation in acid mine drainage. *Geochimica et cosmochimica acta* **2009**, *73*, (5), 1247-1263.
23. Vance, D.; Archer, C.; Bermin, J.; Perkins, J.; Statham, P. J.; Lohan, M. C.; Ellwood, M. J.; Mills, R. A., The copper isotope geochemistry of rivers and the oceans. *Earth and Planetary Science Letters* **2008**, *274*, (1–2), 204-213.
24. Balistrieri, L. S.; Borrok, D. M.; Wanty, R. B.; Ridley, W. I., Fractionation of Cu and Zn isotopes during adsorption onto amorphous Fe(III) oxyhydroxide: Experimental mixing of acid rock drainage and ambient river water. *Geochimica et cosmochimica acta* **2008**, *72*, (2), 311-328.
25. Borrok, D. M.; Nimick, D. A.; Wanty, R. B.; Ridley, W. I., Isotopic variations of dissolved copper and zinc in stream waters affected by historical mining. *Geochimica et cosmochimica acta* **2008**, *72*, (2), 329-344.
26. Bigalke, M.; Weyer, S.; Kobza, J.; Wilcke, W., Stable Cu and Zn isotope ratios as tracers of sources and transport of Cu and Zn in contaminated soil. *Geochimica et Cosmochimica Acta* **2010**, *74*, (23), 6801-6813.
27. Maréchal, C. N.; Télouk, P.; Albarède, F., Precise analysis of copper and zinc isotopic compositions by plasma-source mass spectrometry. *Chemical Geology* **1999**, *156*, (1–4), 251-273.
28. Zhu, X. K.; O'Nions, R. K.; Guo, Y.; Belshaw, N. S.; Rickard, D., Determination of natural Cu-isotope variation by plasma-source mass spectrometry: implications for use as geochemical tracers. *Chemical Geology* **2000**, *163*, (1–4), 139-149.
29. Archer, C., Vance, D., Large fractionations in Fe, Cu, and Zn isotopes associated with Archean microbially-mediated sulphides. In *Goldschmidt Geochim. Cosmochim. Acta Davos, 2002; Vol. 66 (15A)*.
30. Mathur, R.; Titley, S.; Barra, F.; Brantley, S.; Wilson, M.; Phillips, A.; Munizaga, F.; Makshev, V.; Vervoort, J.; Hart, G., Exploration potential of Cu isotope

- fractionation in porphyry copper deposits. *Journal of Geochemical Exploration* **2009**, *102*, (1), 1-6.
31. Schleicher, N. J.; Norra, S.; Chai, F.; Chen, Y.; Wang, S.; Cen, K.; Yu, Y.; Stüben, D., Temporal variability of trace metal mobility of urban particulate matter from Beijing – A contribution to health impact assessments of aerosols. *Atmospheric Environment* **2011**, *45*, (39), 7248-7265.
32. Minguillón, M. C.; Cirach, M.; Hoek, G.; Brunekreef, B.; Tsai, M.; de Hoogh, K.; Jedynska, A.; Kooter, I. M.; Nieuwenhuijsen, M.; Querol, X., Spatial variability of trace elements and sources for improved exposure assessment in Barcelona. *Atmospheric Environment* **2014**, *89*, 268-281.
33. Amato, F.; Viana, M.; Richard, A.; Furger, M.; Prévôt, A. S. H.; Nava, S.; Lucarelli, F.; Bukowiecki, N.; Alastuey, A.; Reche, C.; Moreno, T.; Pandolfi, M.; Pey, J.; Querol, X., Size and time-resolved roadside enrichment of atmospheric particulate pollutants. *Atmos. Chem. Phys.* **2011**, *11*, (6), 2917-2931.
34. Harrison, R. M.; Jones, A. M.; Gietl, J.; Yin, J.; Green, D. C., Estimation of the Contributions of Brake Dust, Tire Wear, and Resuspension to Nonexhaust Traffic Particles Derived from Atmospheric Measurements. *Environmental Science & Technology* **2012**, *46*, (12), 6523-6529.
35. Guéguen, F.; Stille, P.; Dietze, V.; Gieré, R., Chemical and isotopic properties and origin of coarse airborne particles collected by passive samplers in industrial, urban, and rural environments. *Atmospheric Environment* **2012**, *62*, 631-645.
36. Taylor, S. R., Abundance of chemical elements in the continental crust: a new table. *Geochimica et cosmochimica acta* **1964**, *28*, (8), 1273-1285.
37. Wu, Y.-S.; Fang, G.-C.; Lee, W.-J.; Lee, J.-F.; Chang, C.-C.; Lee, C.-Z., A review of atmospheric fine particulate matter and its associated trace metal pollutants in Asian countries during the period 1995–2005. *Journal of Hazardous Materials* **2007**, *143*, (1–2), 511-515.
38. Pribil, M. J.; Wanty, R. B.; Ridley, W. I.; Borrok, D. M., Influence of sulfur-bearing polyatomic species on high precision measurements of Cu isotopic composition. *Chemical Geology* **2010**, *272*, (1–4), 49-54.
39. Mason, T. F. D.; Weiss, D. J.; Horstwood, M.; Parrish, R. R.; Russell, S. S.; Mullane, E.; Coles, B. J., High-precision Cu and Zn isotope analysis by plasma source mass spectrometry Part 1. Spectral interferences and their correction. *Journal of Analytical Atomic Spectrometry* **2004**, *19*, (2), 209-217.
40. Peel, K.; Weiss, D.; Chapman, J.; Arnold, T.; Coles, B., A simple combined sample-standard bracketing and inter-element correction procedure for accurate mass bias correction and precise Zn and Cu isotope ratio measurements. *Journal of Analytical Atomic Spectrometry* **2008**, *23*, (1), 103-110.
41. Arnold, T.; Schönbacher, M.; Rehkämper, M.; Dong, S.; Zhao, F. J.; Kirk, G. J. D.; Coles, B. J.; Weiss, D. J., Measurement of zinc stable isotope ratios in biogeochemical matrices by double-spike MC-ICPMS and determination of the isotope ratio pool available for plants from soil. *Analytical and Bioanalytical Chemistry* **2010**, *398*, (7-8), 3115-3125.
42. Moeller, K.; Schoenberg, R.; Pedersen, R. B.; Weiss, D.; Dong, S., Calibration of the New Certified Reference Materials ERM-AE633 and ERM-AE647 for Copper and IRMM-3702 for Zinc Isotope Amount Ratio Determinations. *Geostandards and Geoanalytical Research* **2012**, *36*, (2), 177-199.
43. Querol, X.; Alastuey, A.; Rodriguez, S.; Plana, F.; Ruiz, C. R.; Cots, N.; Massagué, G.; Puig, O., PM10 and PM2.5 source apportionment in the Barcelona

- Metropolitan area, Catalonia, Spain. *Atmospheric Environment* **2001**, *35*, (36), 6407-6419.
44. Grigoratos, T.; Martini, G., Brake wear particle emissions: a review. *Environ Sci Pollut Res* **2015**, *22*, (4), 2491-2504.
45. Straffelini, G.; Ciudin, R.; Ciotti, A.; Gialanella, S., Present knowledge and perspectives on the role of copper in brake materials and related environmental issues: A critical assessment. *Environmental Pollution* **2015**, *207*, 211-219.
46. Loosmore, G. A.; Cederwall, R. T., Precipitation scavenging of atmospheric aerosols for emergency response applications: testing an updated model with new real-time data. *Atmospheric Environment* **2004**, *38*, (7), 993-1003.
47. Thorpe, A.; Harrison, R. M., Sources and properties of non-exhaust particulate matter from road traffic: A review. *Science of The Total Environment* **2008**, *400*, (1-3), 270-282.
48. Iijima, A.; Sato, K.; Yano, K.; Tago, H.; Kato, M.; Kimura, H.; Furuta, N., Particle size and composition distribution analysis of automotive brake abrasion dusts for the evaluation of antimony sources of airborne particulate matter. *Atmospheric Environment* **2007**, *41*, (23), 4908-4919.
49. Garg, B. D.; Cadle, S. H.; Mulawa, P. A.; Groblicki, P. J.; Laroo, C.; Parr, G. A., Brake Wear Particulate Matter Emissions. *Environmental Science & Technology* **2000**, *34*, (21), 4463-4469.

TOC

